Heliyon 10 (2024) e36715

Contents lists available at ScienceDirect

Heliyon

journal homepage: www.cell.com/heliyon

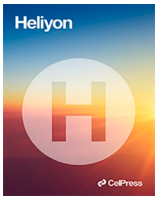

Research article

Synergistic effect of oxygen-rich and hydrogen-rich blast on gas phase in the lower part of blast furnace

Tao Li [a,*], Fangqin Shangguan [a], Guangwei Wang [b,c], Cuiliu Zhang [c], Desheng Li [c]

[a] Steel Industry Green and Intelligent Manufacturing Technology Center, China Iron and Steel Research Institute Group, Beijing, 100081, China
[b] State Key Laboratory of Advanced Metallurgy, University of Science and Technology Beijing, Beijing, 100083, China
[c] School of Metallurgical and Ecological Engineering, University of Science and Technology Beijing, Beijing, 100083, China

ARTICLE INFO

Keywords:
Blast furnace
Oxygen-enhanced blast
Hydrogen-rich metallurgy
CFD

ABSTRACT

The BF(blast furnace) process has become the most powerful pointcut for energy conservation and emission reduction in the iron and steel industry. Few researchers have studied the composition and distribution of bosh gas with co-injection of pulverized coal and natural gas under the oxygen-enriched blast. In this paper, a 3D model of pulverized coal(PC) and natural gas(NG) synergistic combustion was established with a new method of assessment of the utilization rate of bosh gas by using the method of computational fluid dynamics(CFD). The distribution and utilization rate of bosh gas were systematically studied, and the results have shown that when the O2 concentration in the hot blast increased from 27 % to 32 %, the burnout rate of PC increased by 5.08 percentage points, the maximum temperature in the raceway increased by 125K, the residence time of PC particles increased by 0.0017s, the utilization rate of bosh gas increased 2.1 percentage points.

1. Introduction

Iron and steel were important foundational materials for promoting global economic development and social progress, which was still essential material that could not be replaced. In the whole steel production process, the BF-BOF long process was still in the dominant position, accounting for about 55 %, and as high as 90 % in China [1–5]. It was worth noting that 80 % of the heat in the ironmaking process of BF came from the combustion process of coke inside the BF, and the rest came from the physical heat brought in by the hot blast and the chemical heat produced by other fuels [6–9]. In the process of coking, a large amount of waste gas and water would be produced, which would cause great pollution to our living environment. With the exploitation of coal resources, the price of coal was rising day by day, which led to an increase in coking costs. Therefore, it was urgent to find alternative energy sources for coke. Until 1950, based on ensuring the role of the coke column frame, researchers tried to inject other fuels into the BF to reduce the dependence of the BF on coke. According to the distribution of regional resources, fuel injected into blast furnace was also different, the kinds of common fuel injected into BF: NG, coal, waste plastics and heavy oil, BF injection fuel could lead to a wide range of economic and environmental benefits, such as lower production costs, reduce coke consumption and CO_2 emissions, adjust the stability of furnace operation [10–17]. PC is the most widely used BF injection fuel in China at present, and injection technology and equipment transformation has been quite mature, but with the increase of coal ratio in the furnace, there would be a large number of unburned PC particles in the raceway, which would affect the permeability of coke bed, thus affecting the forward stability of BF condition.

* Corresponding author.
E-mail address: Litao0405@hotmail.com (T. Li).

https://doi.org/10.1016/j.heliyon.2024.e36715
Received 23 May 2024; Received in revised form 5 August 2024; Accepted 21 August 2024
Available online 24 August 2024

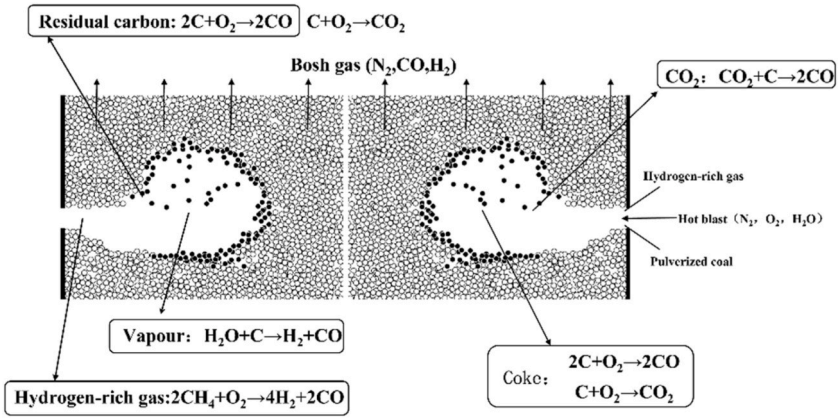

Fig. 1. Main reaction in the low part of BF.

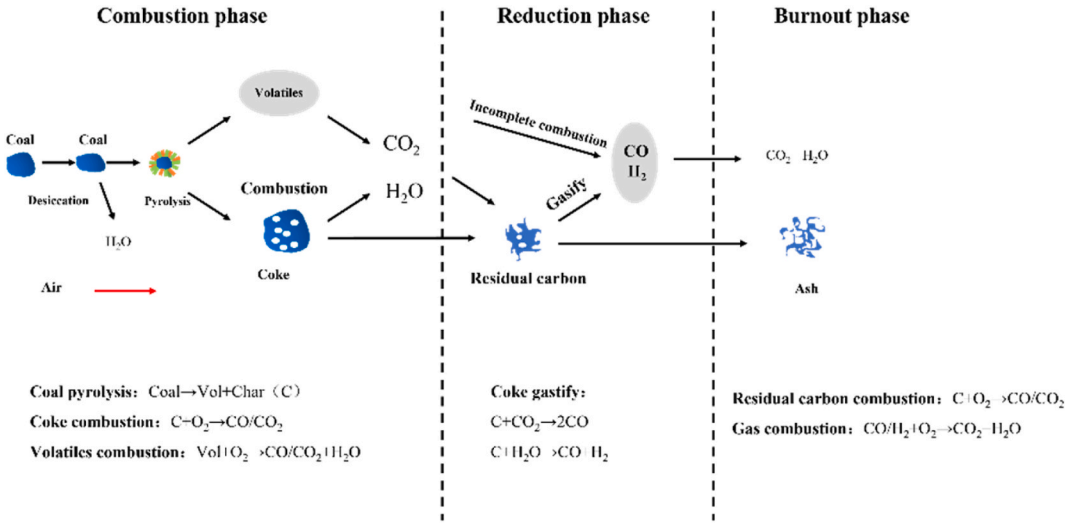

Figure 2. Devolatilization and combustion process of PC particles.

Therefore, the burnout rate of PC in the raceway would limit the further improvement of the coal ratio [15,16]. Countries rich in NG resources, such as the former Soviet Union, North America, Italy, and other countries have carried out industrial trials injecting NG into BF, in an attempt to reduce the dependence of BF iron-making on coke. China first carried out the industrial trial of injection of NG into BF at Chong Steel, which alleviated the shortage of coke resources at that time [18–23]. However, there was no large-scale application of injection of NG into BF in China now, but facing environmental pressure and energy crisis, China was stepping up to the exploitation of NG resources, and putting forward the development of hydrogen metallurgy, further the theory study on the injection NG into BF gas was necessary, for injection of NG into BF and hydrogen reduction in the future practice, and provide theoretical guidance and reference [9]. Previous studies have proved that injecting NG into the BF is more conducive to the stability of the BF condition and could improve the permeability of the BF [22–25]. In addition, compared with solid fuel injection, NG injection into BF has the advantages of easy injection, convenient maintenance of the injection system, and reduction of ash and other particles collision in BF tuyere-raceway and coke bed [26].

Recent industry trends towards decarbonization and stricter emission regulations have also influenced the exploration of alternative fuels. The push for cleaner energy sources and improved emission controls is driving innovation and research in steel production methods, including the integration of NG and hydrogen into the BF process. These trends emphasize the need for sustainable practices and reduction of environmental impact, aligning with global efforts to mitigate climate change and transition to low-carbon technologies.

In China, there was relatively little research on the injection of NG into BF, and the industrial trial of injection of NG into blast furnace has a high cost and long test cycle. Meanwhile, BF was a high-temperature black box, the reaction and atmosphere in the furnace were extremely complex, and it was very difficult to directly observe the atmosphere changes in the BF. The rapid development of computing power and the method of computational fluid dynamics (CFD) have provided an economical, effective, and feasible

Table 1
Basic governing equations of the gas phase.

Mass equations	$\nabla\cdot(\rho U) = \sum_{n_p}\dot{m}$
Momentum equation	$\nabla\cdot(\rho UU) - \nabla\cdot\left[(\mu+\mu_i)\left(\nabla U + (\nabla U)^T\right)\right] = -\nabla\left(P+\frac{2}{3}\rho k\right) + \sum_{n_p} f_D$
Energy equation	$\nabla\cdot\left[\rho UH - \left(\frac{\lambda}{C_p}+\frac{\mu_i}{\sigma_H}\right)\right] = \sum_{n_p} q$
Composition equation	$\nabla\cdot\left[\rho UY_i - \left(\frac{\lambda}{\Gamma_i}+\frac{\mu_i}{\sigma_{Yi}}\right)\right] = W_i$
Turbulent kinetic energy equation	$\nabla\cdot\left[\rho Uk - \left(\mu+\frac{\mu_i}{\sigma_k}\right)\nabla k\right] = P_k - \rho\varepsilon$
Equation of turbulent dissipation rate	$\nabla\cdot\left[\rho U\varepsilon - \left(\mu+\frac{\mu_i}{\sigma_\varepsilon}\right)\nabla\varepsilon\right] = \frac{\varepsilon}{k}(C_1P_k - C_{2\rho\varepsilon})$

Where: ρ–gas density, $kg\cdot m^{-3}$; U–gas velocity, $m\cdot s^{-1}$; n_p–number of particles per unit volume, m^{-3}; $\dot{m}$–particle mass transition rate, $kg\cdot s^{-1}$; μ–dynamic viscosity, $Pa\cdot s^{-1}$; P–pressure, Pa; k–turbulent kinetic energy, $m^2\cdot s^{-2}$; f_D–drag force on particles, N; H–enthalpy, $J\cdot kg^{-1}$; λ–enthalpy, $W\cdot m^{-1}\cdot K^{-1}$; C_p–The specific heat capacity of particles, $J\cdot kg^{-1}\cdot K^{-1}$; q–heat flow rate of particles, W; Y_i–mass fraction of component i; Γ_i–diffusion coefficient of component i, W_i–reaction rate of component i, $kg\cdot m^{-3}\cdot s^{-1}$; σ_k,σ_ε–turbulence model constant; ε–turbulent dissipation rate, $m^2\cdot s^{-3}$; C_μ–empirical constant, 0.09.

method for understanding the bosh gas transport characteristics and combustion behaviour in the raceway of BF. Previous studies have proved the effectiveness of using the CFD method to establish a PC combustion model in BF [27–36]. However, few researchers have studied the utilization of bosh gas by conducting numerical simulation research on the combustion process of co-injection of PC and NG with oxygen-enhanced synergistic combustion in BF. In this paper, a mathematical model was established to reveal the bosh transport characteristics and combustion behaviour in the raceway when co-injection of PC and NG in BF under the condition of oxygen-enhanced synergistic combustion.

2. Model

2.1. Synergistic combustion model

Various complex physical and chemical reactions occurred in the raceway of BF, the main reactions were shown in Fig. 1, which mainly include: (a) turbulent flow of continuous phase (volatile, hot blast, bosh gas, NG); (b) turbulent flow of discrete phase (PC particles) in the continuous phase; (c) combustion of fuel (combustion of volatile and residual carbon); (d) heat, mass and momentum transfer between the continuous phase and the discrete phase. In this paper, the transport characteristics and combustion behaviour of PC and NG in the raceway of BF were simulated by establishing a three-dimensional mathematical model using the method of CFD. Due to the symmetry between different tuyere of the BF, to reduce the computational burden of the model, contours of velocity, temperature, gas phase concentration, and the burnout rate of PC particles in the central symmetry plane of the raceway were obtained, to represent the combustion performance in the whole lower part of the BF [36,37].

2.1.1. Basic assumption

To reduce the computational burden, the complex physical and chemical reactions in the tuyere and raceway of BF were reasonably simplified, and the simplifications are as follows.

(1) By considering PC particles as regular spheres, the computational model can more easily predict their trajectories, velocities, and reactions without the need to solve for complex shapes or irregular geometries. PC was treated as Lagrange discrete phases, and the PC particles as regular spheres;
(2) In the high-temperature and turbulent environment of the raceway, the dominant processes are combustion and gasification rather than collisions and fragmentations, so the collision and fragmentation between different particles of PC and the influence of unburned PC on the whole combustion system were neglected;
(3) For steady-state simulations where the focus is on understanding the average behavior rather than transient phenomena. It was assumed that the operating condition of the BF was stable, and the size of the raceway was fixed with the change in operating conditions.
(4) The introduction of PC and NG significantly affects the overall combustion characteristics, and capturing their behavior provides valuable insights into the combustion dynamics. The coke reaction (combustion/gasification) in the raceway was more complex and only PC and NG combustion was considered;
(5) The water vapor reacts with the residual carbon in the PC particles and is fully mixed with the hot blast, so that the essential interaction between water vapor and carbon could be captured.

2.1.2. Basic control equations

The BF tuyere and raceway were in the turbulent zone with high average Reynolds numbers. The gas flow of the model was

Table 2
Reaction mechanism and rate of pulverized coal and NG.

Reaction	Reaction kinetics
$VM + O_2$=CO_2+$H_2O + N_2$	$A = 2.1e+11\ s^{-1}$; $E = 2.03e+08 J{\cdot}mol^{-1}$
$Char$+$0.5O_2$=CO	$A = 2.1e+11\ s^{-1}$; $E = 2.033 + 08\ J\ mol^{-1}$; $\beta = 0.68$
$Char + CO_2$=$2CO$	$A = 6.783 + 4\ s^{-1}$; $E = 3.63e+08\ J\ mol^{-1}$; $\beta = 0.68$
$Char + H_2O$=$CO + H_2$	$A = 8.55e+4\ s^{-1}$; $E = 3.4e+08\ J\ mol^{-1}$

calculated based on the Reynolds mean Navier-Stokes (RANS) equations, which account for the stochastic variation of the flow characteristics caused by turbulence by decomposing the flow characteristics into the Reynolds stress terms introduced by the mean and wave components. The variables such as velocity, pressure, and concentration of gas phase could be obtained by solving these equations, which monitoring equations are shown in Table 1 [38].

2.1.3. Combustion model

The combustion of PC particles in the tuyere and raceway of BF was a multi-step interactive reaction process. Firstly, N_2 at room temperature was used as the carrier gas to transport PC particles from the coal lance to the tuyere. When the PC particles encounter the high-speed hot blast from the blowpipe, the gas-solid two phases complete the preheating of PC particles through heat transfer. As the temperature of PC particles increased, the PC particles began to devolatilize, resulting in volatile matter and residual carbon. Meanwhile, residue carbon reacted with CO_2 and H_2O through gasification to generate CO and H_2, and combustible gas CO and H_2 combusted with the remaining O_2 to generate CO_2 and H_2O. The specific reaction processes of PC particles in the raceway of BF tuyere were shown in Fig. 2.

(1) Devolatilization

The process of devolatilization of PC was treated as a two-step competition model. The so-called two-step competition model refers to the two devolatilization processes of PC at high temperature and low temperature at two different rates [39]:

Low temperature $\alpha_1 VM_1 + (1\text{-}\alpha_1)C_1$ Equation 2-1

High temperature $\alpha_2 VM_2 + (1 - \alpha_2)C_2$ Equation 2-2

The chemical reaction rate constants of the above two reactions were calculated by the Arrhenius formula:

$$k = A\ \exp(-E / T) \quad 2\text{-}3$$

Devolatilization rate could be expressed as:

$$\frac{dw(VM)}{dt} = (\alpha_1 k_1 + \alpha_2 k_2)C_0 \quad 2\text{-}4$$

Where, k_1 and k_2 were the devolatilization rate of PC under low-temperature and high-temperature conditions respectively; C_0 was the ash removal mass of PC; The preexponential factor and activation energy of the chemical reaction at the two temperatures were respectively: $A_1 = 3.7 \times 10^5 s^{-1}$, $E_1 = 18000$K, $A_2 = 1.46 \times 10^{13} s^{-1}$, $E_2 = 30189$K. α_1- mass fraction of volatile matter in dry ash-free basis, $\alpha_2 = 1.25\alpha_1^2 + 0.92\alpha_1$.

(2) Gas combustion

In this paper, PC volatiles and NG were simply treated as combustible gases. According to the field production data, NG was regarded as a single CH_4, and the molecular formula ($C\alpha H\beta O\gamma N\delta$) of PC volatiles was determined by the characteristics of PC. The vortex dissipation model was adopted for volatile combustion, and the measurement number of volatile combustion reactions was calculated according to the proximate analysis and ultimate analysis of PC [27]:

$$r_i = C_A \frac{\varepsilon}{R} \min\left(\frac{[i]}{v_i'}\right) \quad 2\text{-}5$$

where: r_i –Reaction rate of components i in the volatile matter, mol/(m^3·s); $\frac{\varepsilon}{R}$–The scalar fraction of the time that large vortices exist for material R; v_i'–i Stoichiometry of the components; C_A– constant-4.0;

The combustion of volatile matter ($C_\alpha H_\beta O_\gamma N_\delta$) consists of the following two gas reactions [39]:

$$C_\alpha H_\beta O_\gamma N_\delta + aO_2 \rightarrow bCO + cH_2O + dN_2\ R_1$$

$$CO + 0.5O_2 \rightarrow CO_2\ R_2$$

Gas combustion reaction, in addition to volatile combustion, H_2 combustion also was considered. The expression is:

Table 3
Governing equations of discrete phase.

Mass equation	$\frac{dm_p}{dt} = -\dot{m}$
Momentum equation	$m_p\frac{du_p}{dt} = -f_D$
	$-f_D = \frac{1}{8}\pi d_p^2 \rho C_D \lvert U-U_P\rvert (U-U_P)$
Energy equation	$m_p C_p \frac{dT_p}{dt} = h_{i,conv}A_p(T_g-T_p) + \sum\frac{dm_p}{dt}H_{reac} + A_p\varepsilon_p\sigma_B\left(T_{rad}^4 - T_p^4\right)$

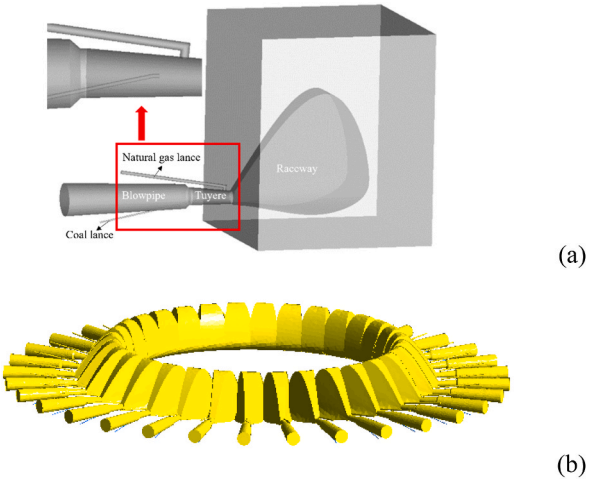

Fig. 3. Model of blowpipe-tuyere-coal/natural-gas lance-raceway.
(a)Single tuyere-raceway model; (b)32 tuyere-raceway model.

$$H_2 + 0.5O_2 \rightarrow H_2O\ R_3$$

Combustion was simulated by (Finite-Rate/Eddy-Dissipation) model, The combustion reaction was simulated by defining the chemical reaction mechanism. The specific combustion mechanism is shown in Table 2 [40].

(3) Oxidation and gasification of residual carbon

After the devolatilization of PC particles, the remaining combustible matter was residual carbon. The Multiple surface reaction model was used to simulate the combustion of residual carbon in PC particles [39]:

$$m_h = \sum \pi d_p^2 \rho Y_{ss} B_s \exp\left(-\frac{E}{RT_P}\right) \quad 2\text{-}6$$

where, m_h-Rate of weight change of the remaining carbon particles, d_p-Diameter of residual carbon particles, ρ-Density of particles, Y_{ss}-The mass fraction of O_2 around the residual carbon. For the oxidation/gasification of residual carbon, a multiphase surface reaction model was used. The oxidation/gasification process of residual carbon mainly included the following reactions (R1-R6), and the reaction rates are shown in Table 2:

$$C(s) + 0.5O_2 \rightarrow CO\ R_4$$

$$C(s) + CO_2 \rightarrow 2CO\ R_5$$

$$C(s) + H_2O \rightarrow CO + H_2\ R_6$$

The governing equations between gas phase and PC particles mainly include mass equation, momentum equation and energy equation. The governing equation of PC particles is shown in Table 3 [39].

where: m_p – Mass of particle, kg; f_D – Drag force of PC particles, N; U_P – Velocity of particles, $m{\cdot}s^{-1}$;U – Velocity of gas, $m{\cdot}s^{-1}$$d_p$ – Diameter of particle, m; C_D – Drag coefficient; T_g – Temperature of gas K; T_P – Temperature of coal particle, K; N_μ – Nusselt number; H_{reac} – Heat of reaction, $J{\cdot}kg^{-1}$;A_p – Particle surface area, m^2;ε_p – Emissivity of particles; I- The intensity of radiation, $W{\cdot}m^{-2}{\cdot}s^{-1}$;$\sigma_B$-Boltzmann's constant.

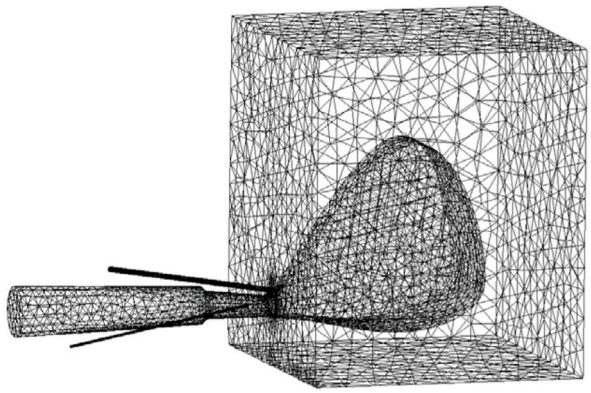

Fig. 4. Mesh of blowpipe-tuyere-coal lance/NG lance-raceway.

Table 4
Proximate analysis and ultimate analysis of PC.

Coal sample	Proximate analysis (wt,%)			Ultimate analysis (wt,%)					HHV(MJ/kg)
	FC_d^a	Ad	Vd	C_{daf}	H_{daf}	O_{daf}	N_{daf}	S_{daf}	
1#	79.60	7.97	12.43	84.55	3.52	1.84	2.02	0.26	33.46

Table 5
Main operation parameters of BF.

Parameters	Value
Number of tuyeres	32
Effective volume of BF/m^3	3200
Blast pressure/KPa	365
O_2 concentration	29 %
Coal ratio/kg/tHM	130
Blast temperature/K	1389
Coal temperature/K	335
Carried gas	N_2

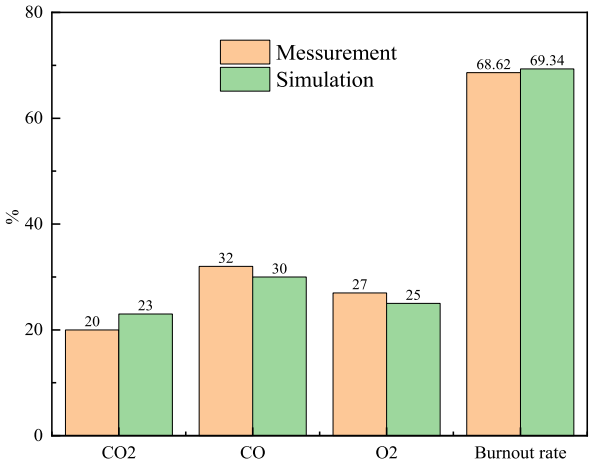

Fig. 5. Model effectiveness comparison results.

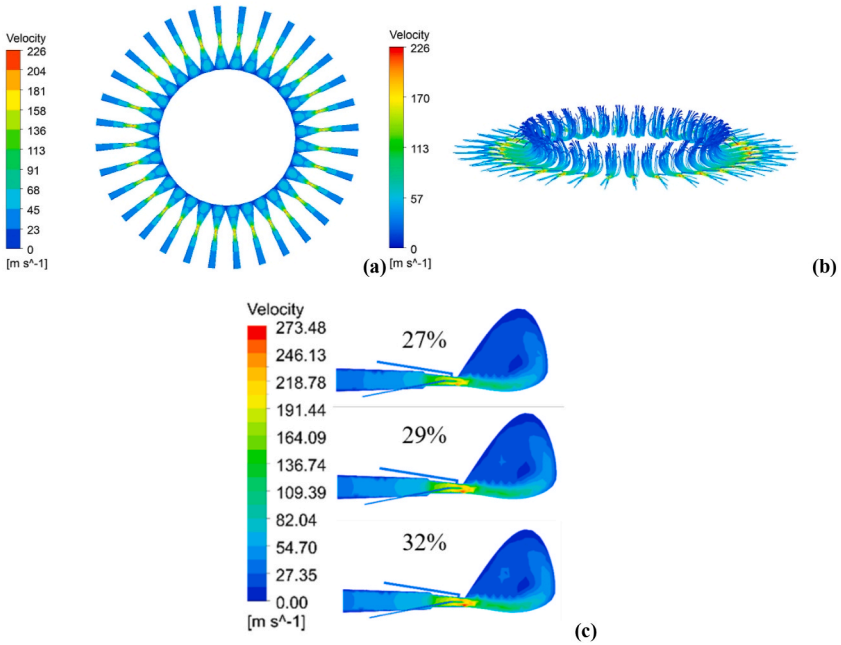

Fig. 6. Transport characteristics of continuous phase in the lower part of BF.
(a)Velocity distribution of transverse central symmetry plane in basic working conditions.
(b)Flow streamline in the lower part of BF under basic operating conditions.
(c)Velocity contours of longitudinal central symmetric plane at different O_2 concentrations.

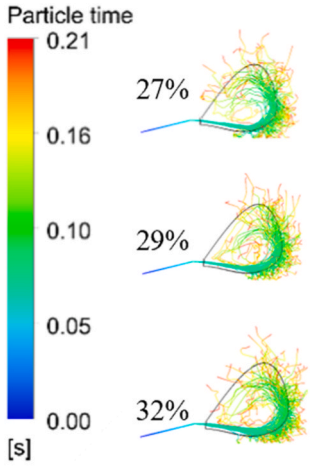

Fig. 7. Trajectories and residence times of PC particles.

2.2. Geometric model and operating conditions

According to the actual BF size, the blowpipe, coal lance, NG lance tuyere and raceway were simplified into a cavity, and the coke bed was simplified into a porous medium. The diameter of the coal lance was 16 mm, the angle of the gun was 13.7°, and the outlet centre of the coal lance was located on the centre line of the tuyere. The PC transport gas was N_2, whose geometric model and geometric parameters are shown in Fig. 3. The mesh division of the model is shown in Fig. 4.

The PC used was taken from the PC injected into the BF of a steel plant. The main parameters of PC, such as proximate analysis and ultimate analysis are shown in Table 4.

Combined with the actual operation parameters of the BF in Table 5, the blast temperature was 1389 K, the coal ratio was 130 kg/tHM, the oxygen concentration in the hot blast was 29 %, the NG injection rate was 74 m^3/t, and the outlet of the lance was taken as the standard working condition on the centre line of the tuyere. Based on the basic operating conditions, as the boundary conditions of

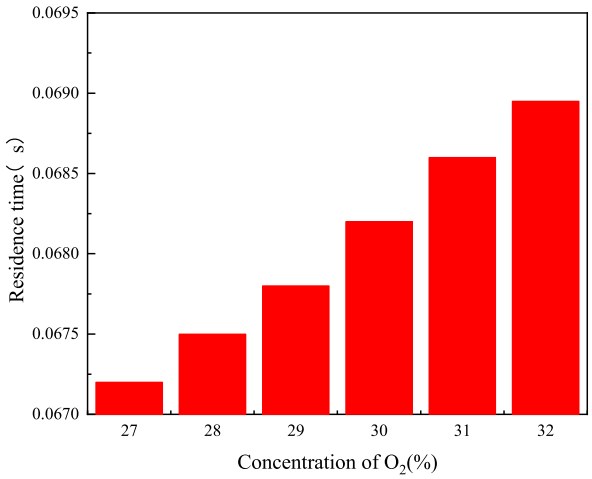

Fig. 8. Residence time of PC particles left the raceway.

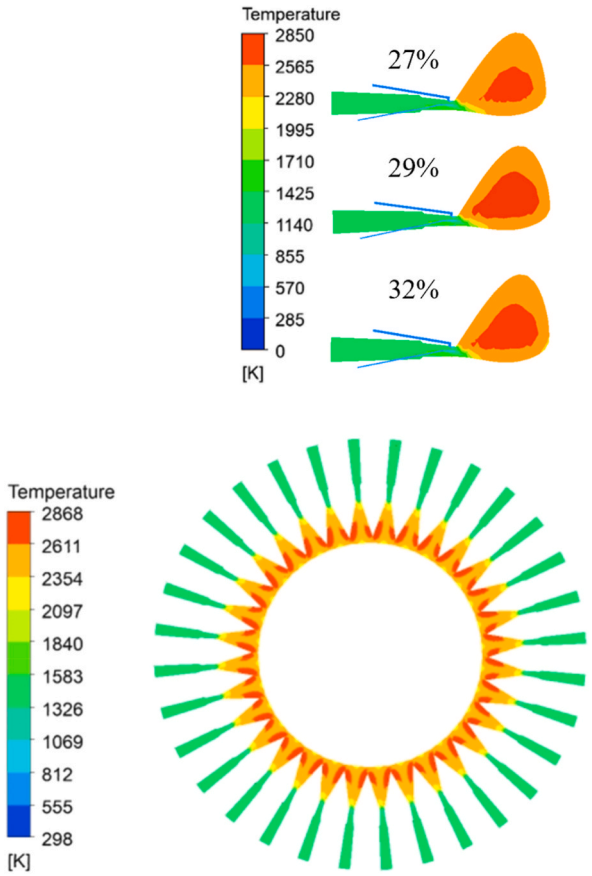

Fig. 9. Temperature distribution of central symmetry plane with different O_2 concentrations.
(a) Temperature distribution in the lower part of the BF under basic conditions.
(b) Temperature distribution in the central symmetry plane of the tuyere-raceway with different O_2 concentrations in hot blast.

simulation calculation, the transport characteristics and combustion behaviours of PC in the raceway were systematically analyzed.

2.3. Validity of the model

To ensure the accuracy and reliability of the calculation results, it was very necessary to study the validity of the model. The previous authors have used CFD to conduct a large number of numerical simulation studies on PC injection in BF, and proved the validity and reliability of the calculation results [31]. Fig. 5 shows the comparison between the simulated value in this model and measurement results when only PC was injected [31]. As could be seen from Fig. 5, the results of the model in this paper were consistent with measurements, both in terms of gas composition and burnout rate of PC, which further proves the effectiveness of the model in this paper.

3. Result

BF was full of CO and presented a reducing atmosphere, oxidizing atmosphere only in the tuyere combustion zone where high temperature blast was blowed in. In this area, PC was simultaneously violently combustion and competed for O_2 in the raceway of BF [40–43].

To study the composition and distribution of bosh gas with co-injection of PC and NG under the condition of an O_2-enhanced blast, it is necessary to study the flow field, temperature, distribution and the burnout rate of PC with O_2 concentration at 27 %, 28 %, 29 %, 30 %, 31 % and 32 %, respectively under the basic operating conditions: blast temperature was 1389 K, coal ratio was 130 kg/tHM.

3.1. Flow field

The velocity distribution and transport characteristics of the continuous phase in the lower part of the BF are shown in Fig. 6. Through Fig. 6(a) and (b), it could be seen that continuous phase velocity distribution and flow characteristics of each tuyere-raceway same, when the hot blast gradually left the blowpipe, the speed of hot blast increased gradually, peaked in tuyere export position, and occurred a large number of backflows. The velocity at the outlet of the tuyere increased significantly, and the high-velocity area in the blowpipe expanded significantly, when the O_2 concentration in the hot blast increased, as shown in Fig. 6(c). The maximum speed reached 246 m/s and 270 m/s respectively when O_2 concentration was 27 % and 32 % in the hot blast, which was caused by the O_2-enhanced strengthened the combustion of PC and NG, releasing more heat. Thus, promoting the devolatilization process of PC particles, volatile concentration in the export of tuyere increased, and a large number of volatile expansion would also increase the speed of the continued phase.

have shown the residence time of PC particles in the raceway of BF with different O_2 concentrations in the blast. As shown in Figs. 7 and 8, with the increase of O_2 concentration in the hot blast, the residence time of PC particles in the raceway gradually increased. When O_2 concentration was 27 %, the residence time of PC particles injected into the lower part of BF was the shortest, which was 0.0672s. With the increase of O_2 concentration, the residence time of PC particles in the raceway increased. When O_2 concentration was 32 %, the residence time of PC particles left the raceway was 0.0689 s. Although the velocity of the gas phase in the blowpipe and tuyere increased, due to the increased with the increase of O_2 concentration in the hot blast, resulting in a decrease of N_2. Thus, the residence time of coal particles increased by the weakening of the transport ability of carried coal particles, which would be more conducive to heat transfer and mass transfer between the PC and hot blast.

3.2. Temperature distribution

As could be seen from Fig. 9, the temperature distribution in the raceway in front of different tuyere was basically the same. With the increase of O_2 concentration in the hot blast, the position of high-temperature area appeared closer to the exit of the coal lance, and the highest temperature in the raceway gradually increased and the high-temperature area gradually expanded. Fig. 10 shows the average gas temperature changed curve along the centre line of the tuyere. The analysis curve has shown that the change of O_2 concentration had little influence on the temperature field in the initial stage of PC combustion. But with the increase of O_2 concentration in the hot blast, the position of high temperature raceway appeared in advance, this is due to the fact that in the initial combustion stage of pulverized coal, the temperature of the pulverized coal particles is low, and it is difficult for oxygen to diffuse into the pulverized coal particles, also, pulverized coal jet is relatively compact, and it is difficult for oxygen to contact the pulverized coal particles in the centre of the pulverized coal jet, The maximum temperature on the centre line of tuyere increased after the coal particles enter the raceway. When the O_2 concentration in the hot blast increased from 27 % to 32 %, the maximum temperature in the raceway increased by 125 K. And the maximum temperature in the raceway increased by 25 K per 1 % increase in the O_2 concentration, this is due to when the pulverized coal jet enters the raceway, the pulverized coal jet is divergent, resulting in sufficient contact between the pulverized coal particles and oxygen. The higher the oxygen concentration, the more fully the contact, and the higher the high-temperature area is caused in advance, also, A higher concentration of oxygen means that the relative amount of nitrogen in the drum will also be reduced, which will take away more heat.

In addition, it could be seen from Fig. 6, as PC particles were preheated and devolatilized when carrier gas and PC particles entered the tuyere and raceway, the gas phase velocity decreased, and the combustion space of PC and NG became larger, pulverized coal particles have more sufficient contact with O_2. Otherwise, with the increase of the temperature of PC particles, the mass transfer between O_2 and PC particles became faster. Meanwhile, with the increase of O_2 concentration in hot blast, the combustion rate of

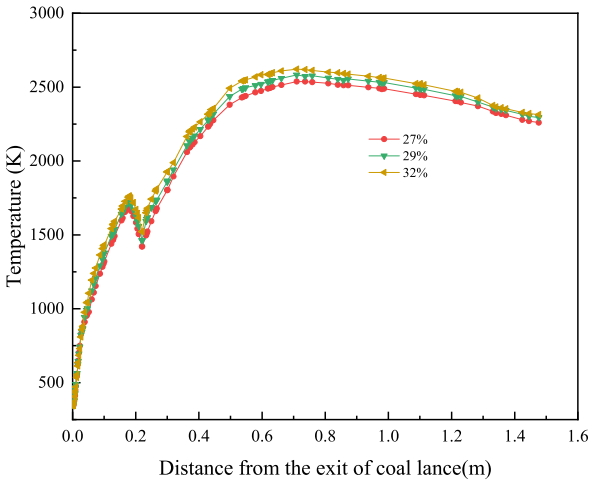

Fig. 10. Gas temperature along the centre line of tuyere with different O_2 concentrations.

volatile and NG was accelerated, which would promote the advanced combustion of residual carbon so that the gas phase temperature increased. However, the increase in the concentration of O_2 reduced the concentration of N_2 in the hot blast so that the heat carried out by N_2 also decreased. In summary, with the increase of O_2 concentration, the maximum temperature in the raceway was higher, and the high-temperature area became larger and closer to the coal lance, which was complementary to the AFT reduction caused by NG injection.

3.3. Gas phase

Fig. 11 shows the effect of O_2 concentration in hot blast on the gas phase composition in the tuyere-raceway of BF. With the increase of O_2 concentration in the hot blast, the concentrations of CO_2, CO, H_2 and H_2O at the same distance from the exit of the coal lance gradually increased. It could also be seen from Fig. 12 that the corresponding high concentration area of CO_2, CO, H_2 and H_2O in the BF raceway enlarged significantly. The higher O_2 concentration in the hot blast resulted in the NG being combusted more fully and released more heat at the tuyere outlet, which further promoted the process of devolatilization of PC and produced more volatile. The combustion of volatile and NG generated more H_2O and CO_2. Meanwhile, higher H_2 o and CO_2 concentrations in turn promoted the gasification of residual carbon, resulting in more CO and H_2 production. As could be seen from Fig. 12, H_2 and CO appeared higher concentration area with the increase of O_2 concentration at the edge of the raceway, so more H_2 and CO would enter the coke bed. Such high reducibility and large area of gas composition would be more conducive to the reduction of iron ore and the combustion and gasification of PC.

3.4. Burnout rate

PC burnout rate was an important index to evaluate the combustion behaviour of PC in the tuyere and raceway of BF, which represented the mass loss caused by volatile combustion and oxidation and gasification of residual carbon, and the calculation formula has shown in Equations (3)–(1) [27]. A large amount of unburned fuel particles entering the coke bed would seriously affect the permeability of the coke bed and affect the condition of the BF. Therefore, it was very necessary to study the burnout rate of PC. Fig. 13 has shown the changed curves of PC burnout rate when O_2 concentration in hot blast was 27 %, 29 % and 32 %. It could be seen from Fig. 13 that O_2-enhanced blast had a very significant influence on the burnout rate of PC in the raceway, and the combustion of PC and NG was intensified due to the increase of O_2 concentration in the hot blast. When the O_2 concentration in the hot blast increased from 27 % to 32 %, the burnout rate of PC increased from 65.28 % to 70.36 %, which also means that under the conditions of oxygen-rich mixed injection of pulverized coal and natural gas, the use of 1t of pulverized coal will reduce CO2 emissions by 0.21t compared to the traditional process.

The reason for the increase in burnout rate is mainly due to, with the increase of O_2 concentration in the hot blast, the concentration of O_2 around the PC particles also increased, which was very beneficial to the combustion of PC. Meanwhile, the increase of O_2 concentration in the hot blast would bring adverse effects, due to the volatilization of PC need to absorb heat from the hot blast, PC and surrounding low-temperature O_2 would hinder the heat transfer between hot blast and PC particles, which was not conducive to the volatilization of coal particles and preheating, also, due to the limited amount of unburned coal powder, the promotion of pulverized coal combustion is also limited by the increase of the concentration of immediate oxygen. It could be seen from Fig. 14 that with the increase of concentration of O_2, The promotion of PC combustion was weakened.

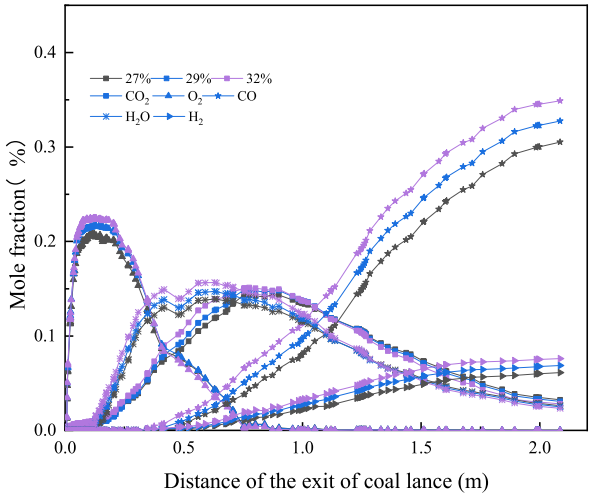

Fig. 11. Distribution of gas in the center line of tuyere with different O_2 concentrations.

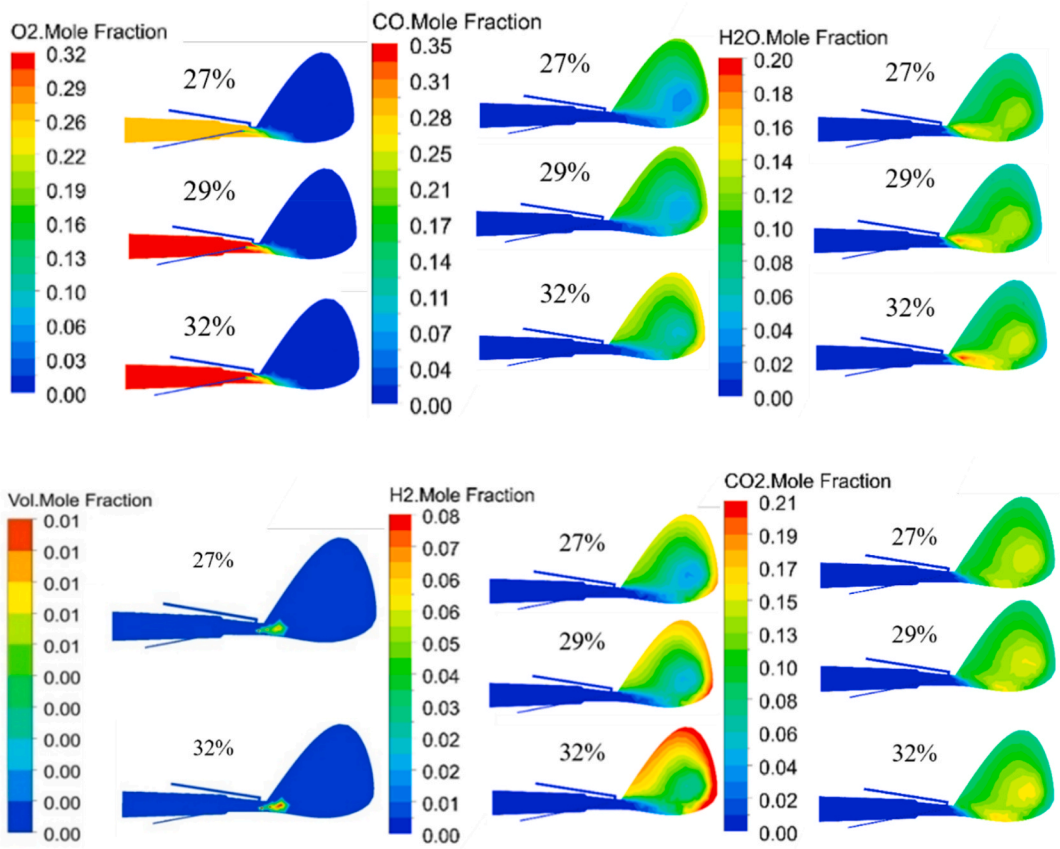

Fig. 12. Gas distribution in the symmetry plane at different O_2 concentrations.

$$Burnout = \frac{1 - \frac{X_{a,0}}{X_a}}{1 - X_{a,0}} \times 100\% \qquad \text{Equation 3-1}$$

where: $X_{(a,0)}$- Mass fraction of ash in the original particle;X_a- Particle mass fraction of ash in this state.

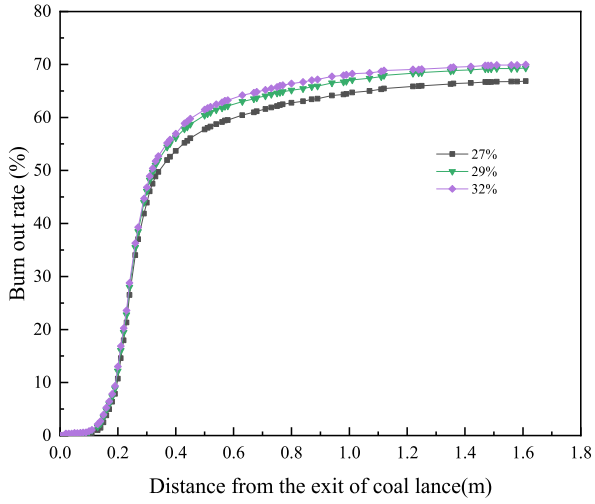

Fig. 13. Coal burnout rate with different O_2 concentration in the center line of tuyere.

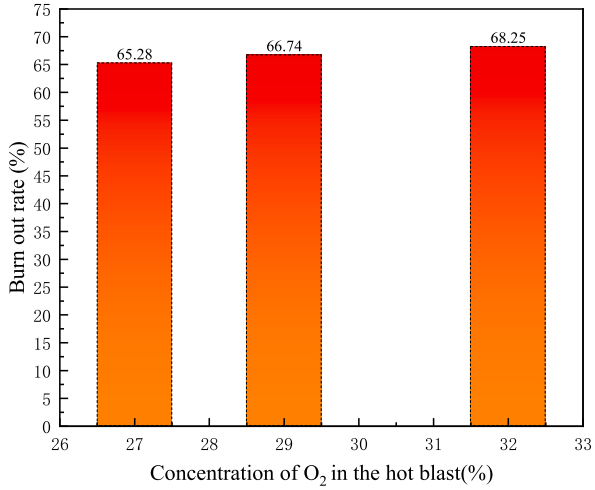

Fig. 14. Burnout rate of PC at the outlet of raceway with different O_2 concentrations.

3.5. Utilization of bosh gas

The utilization rate of BF gas was an important parameter to measure the energy consumption level of BF. Increasing the utilization rate of high gas was not only beneficial to the indirect reduction of iron ore but also beneficial to further reduce the fuel ratio. Studies have shown that the fuel ratio decreases by 1.2 % for every percentage point increase in gas utilization rate [44]. In this paper, the relative content of reducing atmosphere in the raceway was reflected by defining the bosh gas utilization rate η_{CO+H2} in the raceway. Furthered indirectly reflects the BF gas utilization rate, as shown in formula 3-2:

$$\eta_{CO+H2} = \frac{\omega_{CO}+\omega_{H_2}}{\omega_{CO}+\omega_{H_2}+\omega_{CO_2}} \times 100\% \qquad \text{Equation 3-2}$$

where: ω_{CO}-the concentration of CO; ω_{H_2}-the concentration of H_2; ω_{CO_2}-the concentration of CO_2.

Fig. 15 shows the bosh gas utilization rate with different O_2 concentrations along the centre line of the tuyere. It could be seen from Fig. 13 that as the gas gradually moved away from the tuyere, O_2 was gradually consumed and the bosh gas utilization rate gradually increased. With the increase of O_2 concentration in the hot blast, the bosh gas utilization rate at the same position away from the tuyere gradually increased. In addition, it could be seen from Fig. 15 that the O_2 concentration in the blast had little influence on the bosh gas utilization rate at the outlet of the tuyere and the raceway, but had a great influence on the bosh gas utilization rate at the centrecentre of the raceway. Fig. 16 shows the bosh gas utilization rate when the gas left the raceway, as shown in Fig. 16, when the O_2 concentration in the hot blast increased from 27 % to 32 %, the bosh gas utilization rate increased from 91.8 % to 93.9 % when the gas left raceway. Therefore, co-injection of PC and NG into BF would be more conducive to improving the utilization rate of bosh gas and

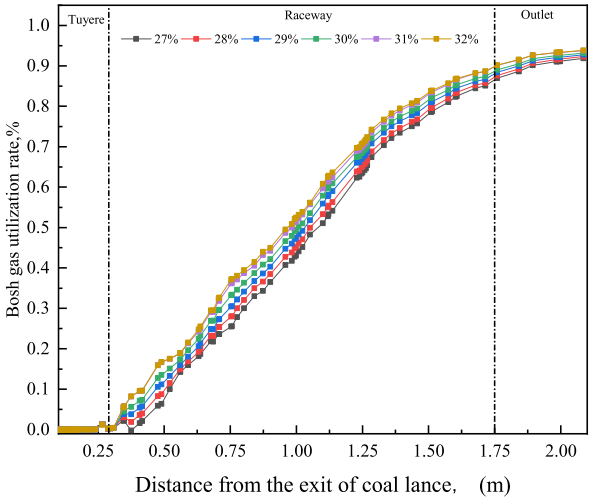

Fig. 15. Utilization rate of bosh gas with different O_2 concentration.

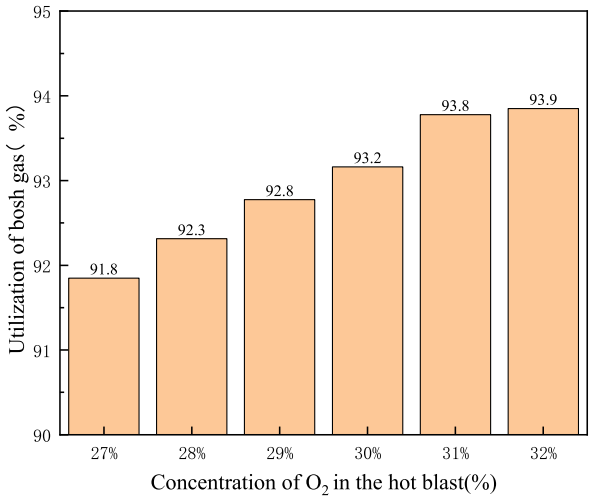

Fig. 16. Utilization rate of bosh gas with different O_2 concentration left the raceway.

indirect reduction of iron ore.

4. Conclusion

In this paper, a 3D model of PC and NG synergistic combustion was established by using CFD. Through the study on the synergistic combustion of PC and NG by O_2-enhanced blast, when the O_2 concentration in the blast increased from 27 % to 32 %, the following conclusions were obtained.

1) The velocity of the gas phase at the outlet of the tuyere increased from 246 m/s to 270 m/s, and the residence time of PC particles in the raceway increased from 0.0672s to 0.0689s, which was more conducive to the heat and mass transfer between PC particles and hot blast.
2) The high-temperature area in the raceway tended to be close to the outlet of the coal lance, and the maximum temperature in the raceway increased by 125 K, which could compensate for the temperature drop caused by NG injection to a certain extent.
3) A larger area and higher concentration of CO, CO_2, H_2 and H_2O were generated in the raceway, and the bosh gas utilization rate increased by 2.1 percentage points when the gas left the raceway, which was conducive to the reduction of iron ore and the utilization rate of BF gas.
4) The burnout rate of PC increased from 65.28 % to 70.36 %, and the influence of O_2-enhanced blast on burning rate gradually weakened with the increase of O_2 concentration in hot blast.

Overall, these findings have significant implications for the iron and steel industry, particularly in optimizing blast furnace operations to improve efficiency and reduce emissions. Additionally, the findings support the use of oxygen-enhanced blast as a viable strategy to compensate for the temperature drop associated with NG injection, ensuring consistent thermal conditions in the furnace.

CRediT authorship contribution statement

Tao Li: Methodology, Investigation, Funding acquisition, Formal analysis, Data curation. **Fangqin Shangguan:** Formal analysis, Data curation. **Guangwei Wang:** Funding acquisition. The main contribution of Cuiliu Zhang and Desheng Li to this paper is to revise and improve the content of this paper.

Declaration of competing interest

The authors declare that they have no known competing financial interests or personal relationships that could have appeared to influence the work reported in this paper.

Acknowledgement

This work was supported by the National Natural Science Foundation of China (nos. S2074029, 1804026) and the USTB-NTUT Joint Research Program (no. 6310063).

References

[1] WorldSteel Association, World Steel in Figures 2001 to 2021[R], World Steel Association, Brussels, 2001-2021.
[2] R.Y. Yin, Metallurgical Process Engineering[M], Metallurgical Industry Press, Bei Jing, 2009.
[3] F.Q. Shangguan, Z.D. Liu, R.U. Yin, Research on the implementation path of carbon peaking and carbon neutrality in steel industry[C], in: Proceedings of the 13th China Iron and Steel Annual Conference, 2022, p. 163.
[4] F.Q. Shangguan, Z.D. Liu, R.U. Yin, Research on the implementation path of "carbon peak" and "carbon neutrality" in steel industry[J], China Metallurgical 31 (9) (2021) 15–20.
[5] F.Q. Shangguan, R.Y. Yin, Y. Li, J.C. Zhou, X.P. Li, On the strategic significance of developing all scrap electric furnace process in China, Iron Steel 56 (8) (2021) 86–92.
[6] C.D. Zhou, J.L. Xu, C.Y. Liu, Suggestions on promoting the development of ironmaking technology in China, Ironmaking 22 (6) (2003) 1–2.
[7] X.C. Li, B. Li, Low carbon transition path of China's iron and steel industry under global temperature-control target, Iron Steel 54 (2019) 224–231.
[8] G.Y. Wen, Discussion on injection of natural gas into blast furnace, Ironmaking (2) (1987) 22–26.
[9] Y. Qingyao, S. Long, C. Lin, et al., Prospect on Injecting Waste Tires into Blast furance[J], World Iron & Steel, 2012.
[10] T. Saeki, S. Nagataki, Change in compressive strength of mortar with fly ash and blast-furance slag powder due to carbonation, Fuel Energy Abstr. 37 (6) (1996) 422.
[11] H. Reintjes, S. Tamura, Injection and combustion of coal in a blast furnace, Iron Steel Eng. 60 (2) (1983) 33–37.
[12] T. Ohji, J. Matyá, N.J. Manjooran, et al., Advances in materials science for environmental and energy technologies III (Ohji/Advances), Injection of BOF dust into the blast furance through tuyere[J] (2014).
[13] S. Raygan, H. Abdizadeh, A.E. Rizi, Evaluation of four coals for blast furnace pulverized coal injection, J. Iron Steel Res. Int. 17 (3) (2010) 8–20.
[14] J.L. Zhang, G.W. Wang, J.G. Shao, et al., Pulverized coal combustion of nitrogen free blast furnace, J. Iron Steel Res. Int. 20 (3) (2013) 1–5.
[15] S. Ren, J.L. Zhang, W.J. Liu, et al., Investigation on fusibility of blast-injection coal ash, J. Iron Steel Res. Int. (2012).
[16] K. Yamaguchi, H. Ueno, K. Tamura, Maximum Injection rate of pulverized coal into blast furnace through tuyeres with consideration of unburnt char, ISIJ Int. 32 (6) (2007) 716–724.
[17] A.K. Silaen, T. Okosun, Y. Chen, et al., Investigation of high rate natural gas injection through various lance designs in a blast furnace, Iron Steel Technol. 1 (3) (2015) 1536–1549.
[18] P. Chris, Pistorius, et al., Increased Use of Natural Gas in Blast Furnace Ironmaking[J], Iron & Steel Technology, 2015.
[19] A. Murao, K. Fukada, H. Matsuno, et al., Effect of natural gas injection point on combustion and gasification efficiency of pulverized coal under blast furnace condition, Tetsu-To-Hagane 104 (5) (2018) 243–252.
[20] K. Halim, Theoretical approach to change blast furnace regime with batural gas injection, J. Iron Steel Res. Int. 20 (9) (2013).
[21] GG Galiev, VI Krivonosov, FP Ponomarev, et al. Blowing-in a blast furnace with natural gas[J]. 976, 20(2):98-101.
[22] SA,Sharadzenidze, NV Kashakashvili, PP Gladkoskok, et al. Blast-furnace operation utilizing natural gas[J]. 1962, 6(9):398-402. .
[23] TL Guo, MS Chu, ZG Liu, et al. Mathematical simulation of rotary area of blast furnace gas injection tuyere [C]. 2012 national iron making production technology conference and iron making academic annual conference proceedings (Part 2). China meeting, 2012:52-57. .
[24] J. Tang, M.S. Chu, F. Li, C. Feng, Z.G. Liu, Y.S. Zhou, Development and progress on hydrogen metallurgy, Int. J. Miner. Metall. Mater. 27 (6) (2020) 713–723.
[25] M.S. Chu, H. Nogami, J.I. Yagi, Numerical analysis on injection of hydrogen bearing materials into blast furnace, ISIJ Int. 44 (5) (2004) 801–808.
[26] Y.S. Shen, B.Y. Guo, A.B. Yu, et al., A three-dimensional numerical study of the combustion of coal blends in blast furnace, Fuel 88 (2) (2009) 255–263.
[27] Y.S. Shen, B.Y. Guo, A.B. Yu, et al., Three-dimensional modelling of coal combustion in blast furnace, ISIJ Int. 48 (6) (2008) 777–786.
[28] C.L. Zhang, G.W. Wang, X.J. Ning, J.L. Zhang, C. Wang, Numerical simulation of combustion behaviors of hydrochar derived from low-rank coal in the raceway of blast furnace, Fuel 278 (2020) 1–8.
[29] Y.R. Liu, Y.S. Shen, Combined experimental and numerical study of charcoal injection in a blast furnace: effect of biomass pretreatment, Energy Fuels 34 (1) (2020) 827–841.
[30] Y.S. Shen, A.B. Yu, P. Zulli, CFD modelling and analysis of pulverized coal injection in blast furnace: an overview, Steel Res. Int. 82 (5) (2011) 532–542.
[31] Y.S. Shen, B.Y. Guo, A.B. Yu, P.R. Austin, P. Zulli, Three-dimensional modelling of infurnace coal/coke combustion in a blast furnace, Fuel 90 (2) (2011) 728–738.
[32] Y.S. Shen, A.B. Yu, P.R. Austin, P. Zulli, CFD study of in-furnace phenomena of pulverised coal injection in blast furnace: effects of operating conditions, Powder Technol. 223 (2012) 27–38.
[33] W. Walker, M. Gu, Selvarasu SK. Ubhayakar, D.B. Stickler, et al., Rapid devolatilization of pulverized coal in hot combustion gases 16 (1) (1977) 427–436.
[34] J.M. Burgess, Fuel combustion in the blast furnace raceway zone, Prog. Energy Combust. Sci. 11 (1) (1985) 61–82.
[35] J.G. Mathieson, J.S. Truelove, H. Rogers, Toward an understanding of coal combustion in blast furnace tuyere injection, Fuel 84 (10) (2005) 1229–1237.
[36] Tao Li, G.W. Wang, H. Zhou, et al., Numerical simulation study on the effects of co-injection of pulverized coal and hydrochar into the blast furnace, Sustainability (2022) 14.
[37] J.L. Zhang, K.C. Zhu, L.X. Zhou, Phase energy equation of pulverized coal in gas-solid multiphase reaction flow, Mechanics and Practice 24 (3) (2002) 3.

[38] S.S. Xu, L.J. Li, R.S. Huang, et al., Simulation study on the best Tertiary air velocity of coal blend combustion in a calciner, Guocheng Gongcheng Xuebao/The Chinese Journal of Process Engineering 13 (2) (2013) 181–185.
[39] Q. Wang, E. Wang, Numerical investigation of the influence of particle shape, pretreatment temperature, and coal blending on biochar combustion in a blast furnace, Fuel: A journal of fuel science (2022), 313-Apr.1.
[40] X.H. Zhang, H.F. Li, W.R. Xu, Z.S. Zou, Development of mathematical model for theoretical Combustion temperature of hydrogen rich blast furnace, J. Mater. Metall. 21 (1) (2022) 31–36.
[41] H.B. Chen, Z. Li, S. Wang, et al., Study on calculation method of theoretical combustion temperature of blast furnace tuyere [C], Metallurgical Engineering Science Forum (2010).
[42] C.L. Zhang, L. Vladislav, R. Xu, et al., Blast furnace hydrogen-rich metallurgy-research on efficiency injection of natural gas and pulverized coal, Fuel 311 (2022) 122412.
[43] C.S. Liu, S.J. Li, H.Y. Tang, Y.W. Gao, Improvement of theoretical combustion temperature calculation model for blast furnace tuyere, J. Northeast. Univ. (Nat. Sci.) 36 (3) (2015) 392–396.
[44] Z.G. Hu, Practice of improving gas utilization rate of No. 5 Blast furnace of Wisco, Wu steel technology 50 (2) (2012) 8–11.